

Hematopoietic stem cell loss and hematopoietic failure in severe aplastic anemia is driven by macrophages and aberrant podoplanin expression

Amanda McCabe,^{1*} Julianne N.P. Smith,^{1**} Angelica Costello,¹ Jackson Maloney,¹ Divya Katikaneni¹ and Katherine C. MacNamara¹

¹Department for Immunology and Microbial Disease, Albany Medical College, NY, USA

*AM and JNPS contributed equally to this work. *Current address: Boston Children's Hospital, Division of Hematology/Oncology, Harvard Medical School, Karp Family Research Lab, Boston, MA, USA. **Current address: Case Western Reserve University, Department of Medicine, Wolstein Research Building, Cleveland, OH, USA*

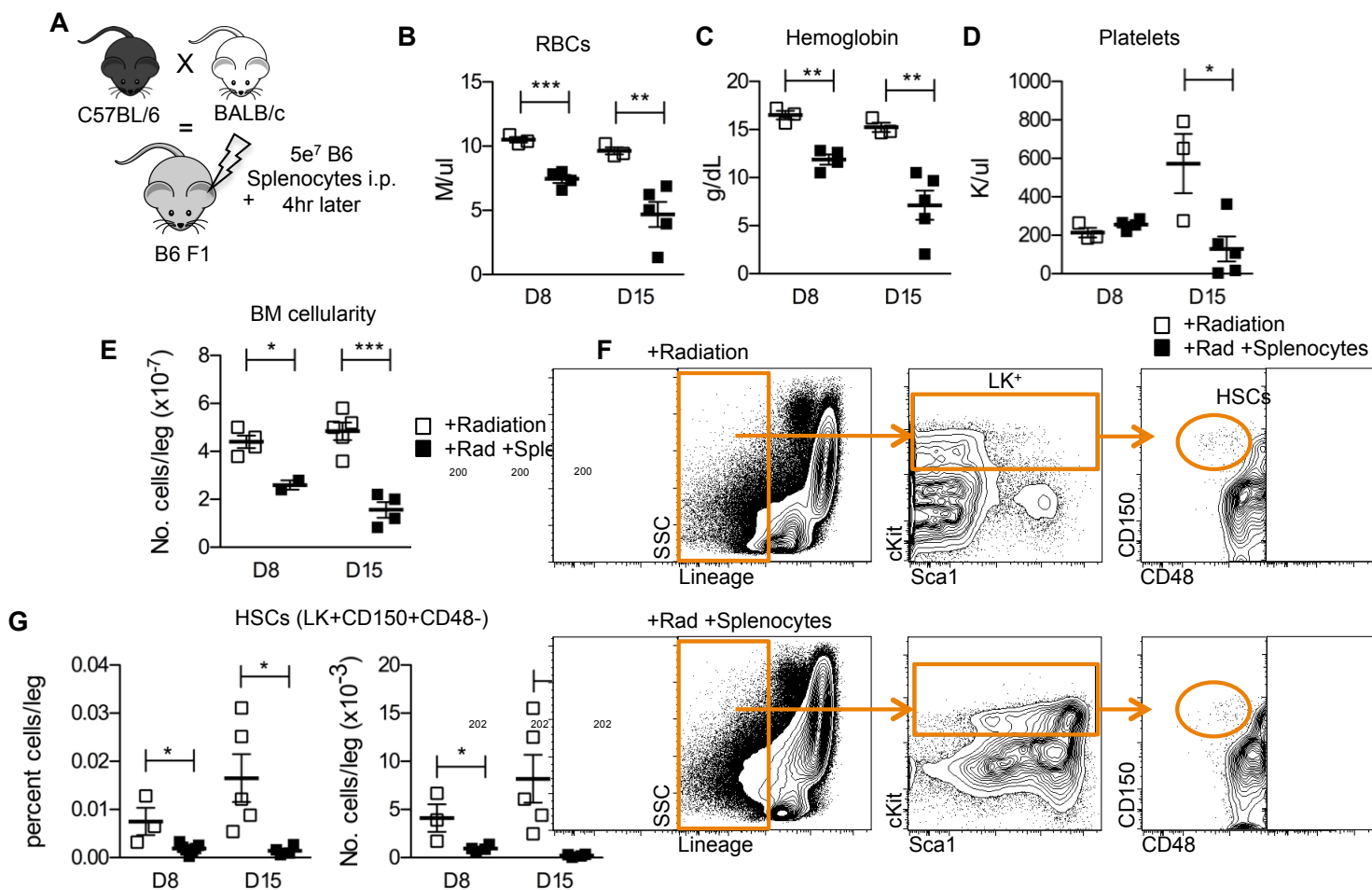
©2018 Ferrata Storti Foundation. This is an open-access paper. doi:10.3324/haematol.2018.189449

Received: January 30, 2018.

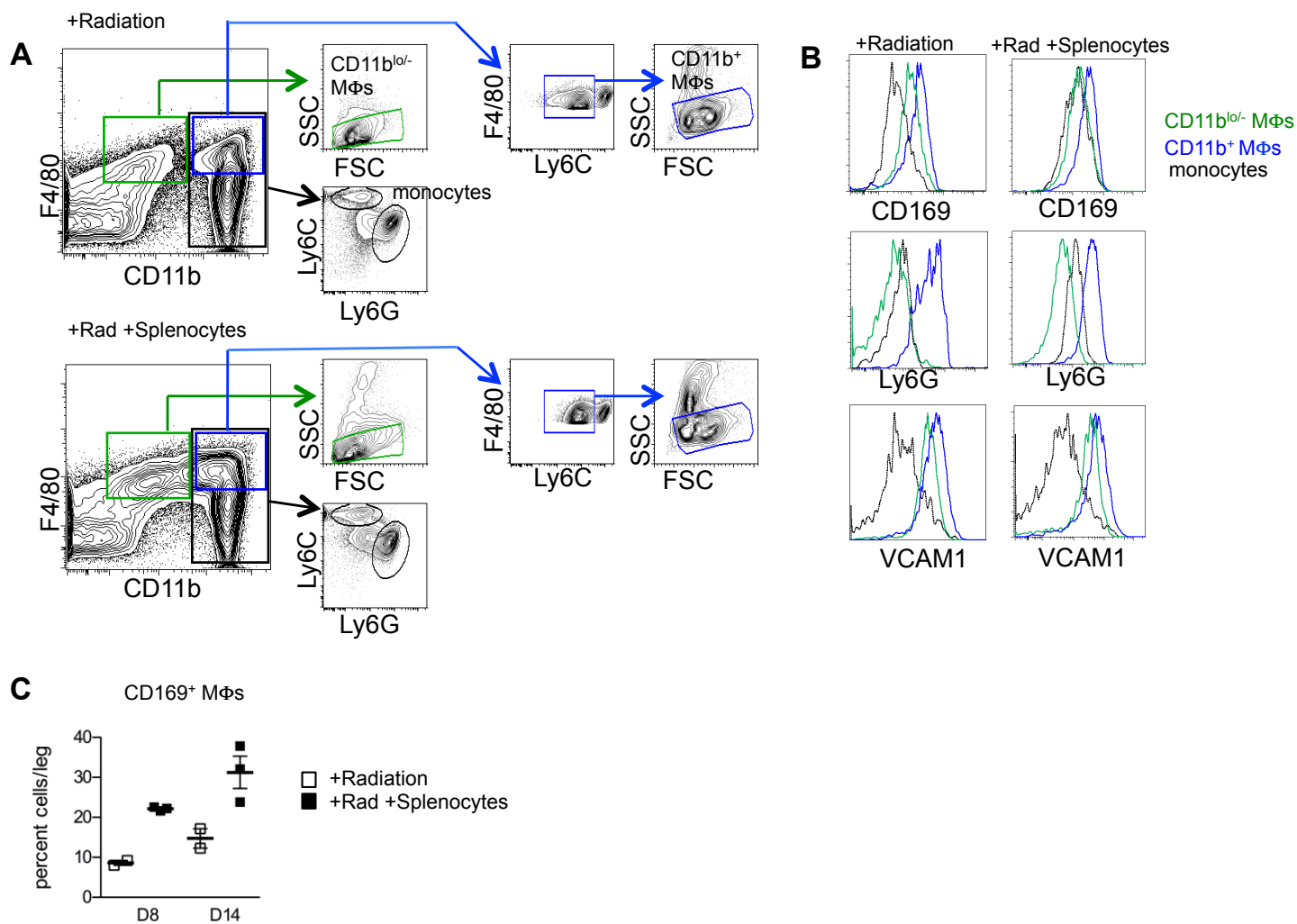
Accepted: May 14, 2018.

Pre-published: May 17, 2018.

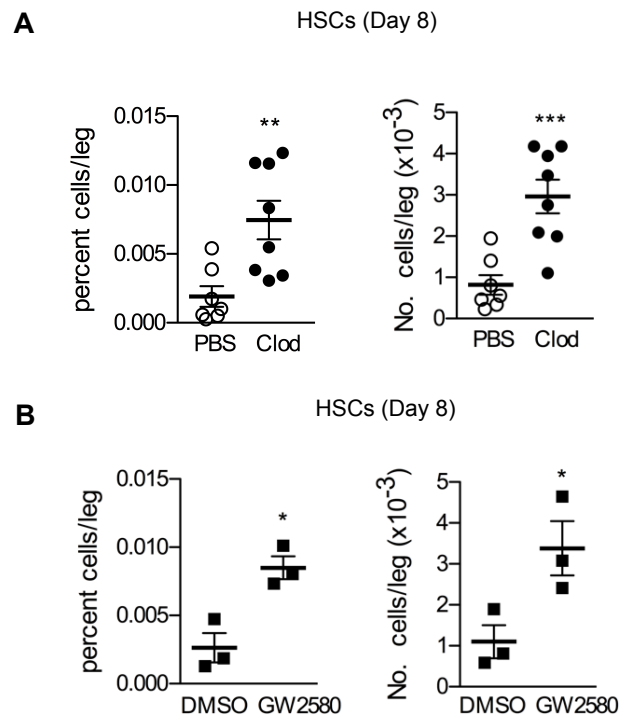
Correspondence: macnamk@amc.edu



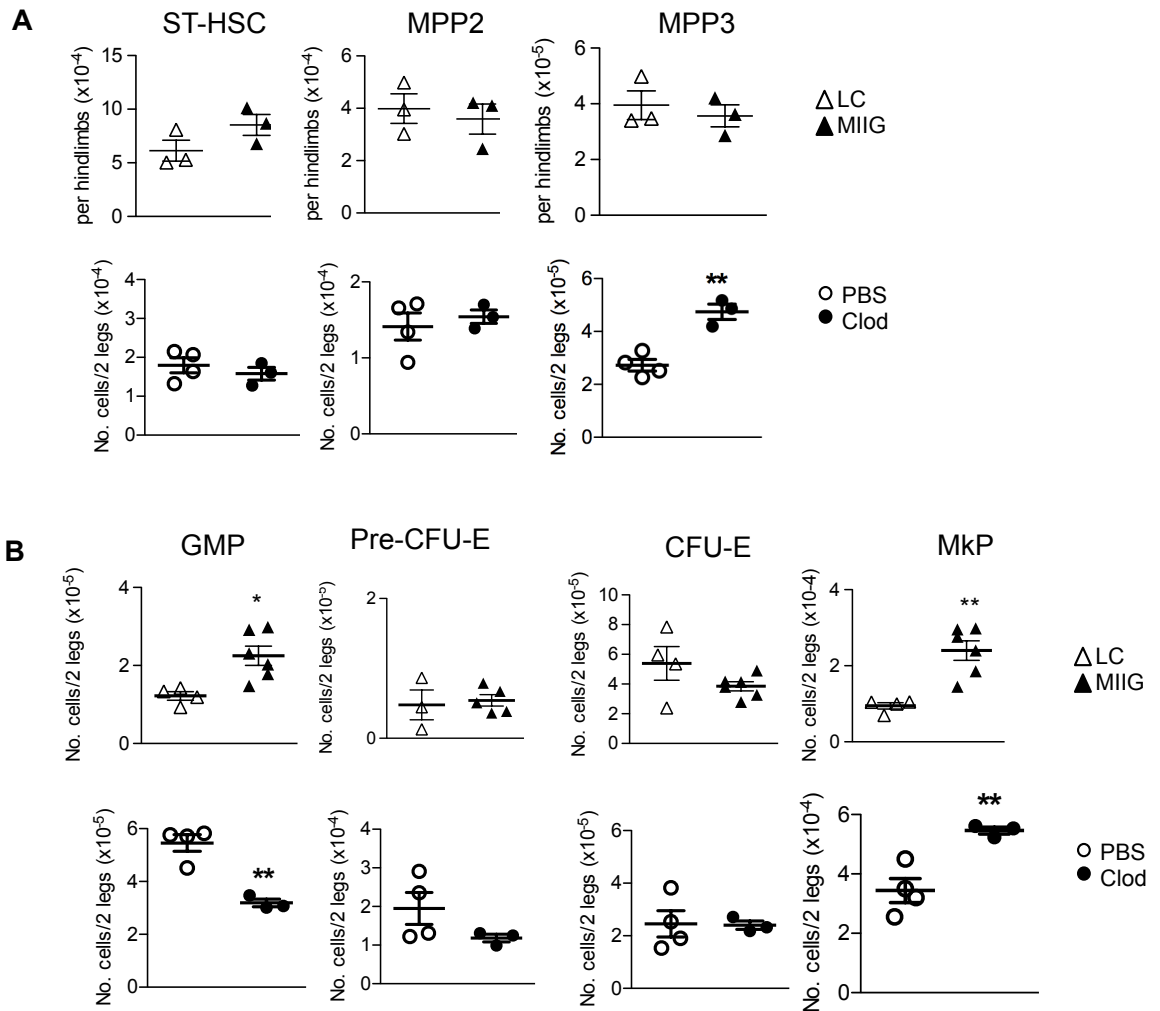
Supplemental Figure 1. Cytopenias and hematopoietic stem cell loss in severe aplastic anemia. **(A)** Schematic showing the generation of a mouse model of severe aplastic anemia (SAA), whereby, C57BL/6 ($H^{b/b}$) and BALB/c ($H^{d/d}$) mice were crossed and F1 progeny ($H^{b/d}$) were induced via sublethal irradiation (300 RADs) and adoptive transfer of 5×10^7 C57BL/6 splenocytes by intraperitoneal (i.p.) injection. Analysis was performed 8 and 15 days post-radiation (+Rad: □) or post-radiation and splenocyte transfer (■). **(B)** Red blood cells, **(C)** hemoglobin, and **(D)** platelets were analyzed in the blood by complete blood count. **(E)** Graph represents bone marrow (BM) cellularity. **(F)** Plots represent gating of hematopoietic stem cells (HSCs) from radiation control (top) and SAA (+Rad +Splenocytes; bottom) mice. **(G)** Absolute frequency and number of HSCs ($LK^+ CD150^+ CD48^-$) in the BM of radiation control (□) and SAA (■) mice at days 8 and 15. Data represent one experiment repeated at least twice with 3-6 mice/group. The mean \pm SEM is shown. Two-tailed student's t-test was used to compare between radiation control and splenocyte-induced mice * $p < 0.05$, ** $p < 0.01$, *** $p < 0.001$.



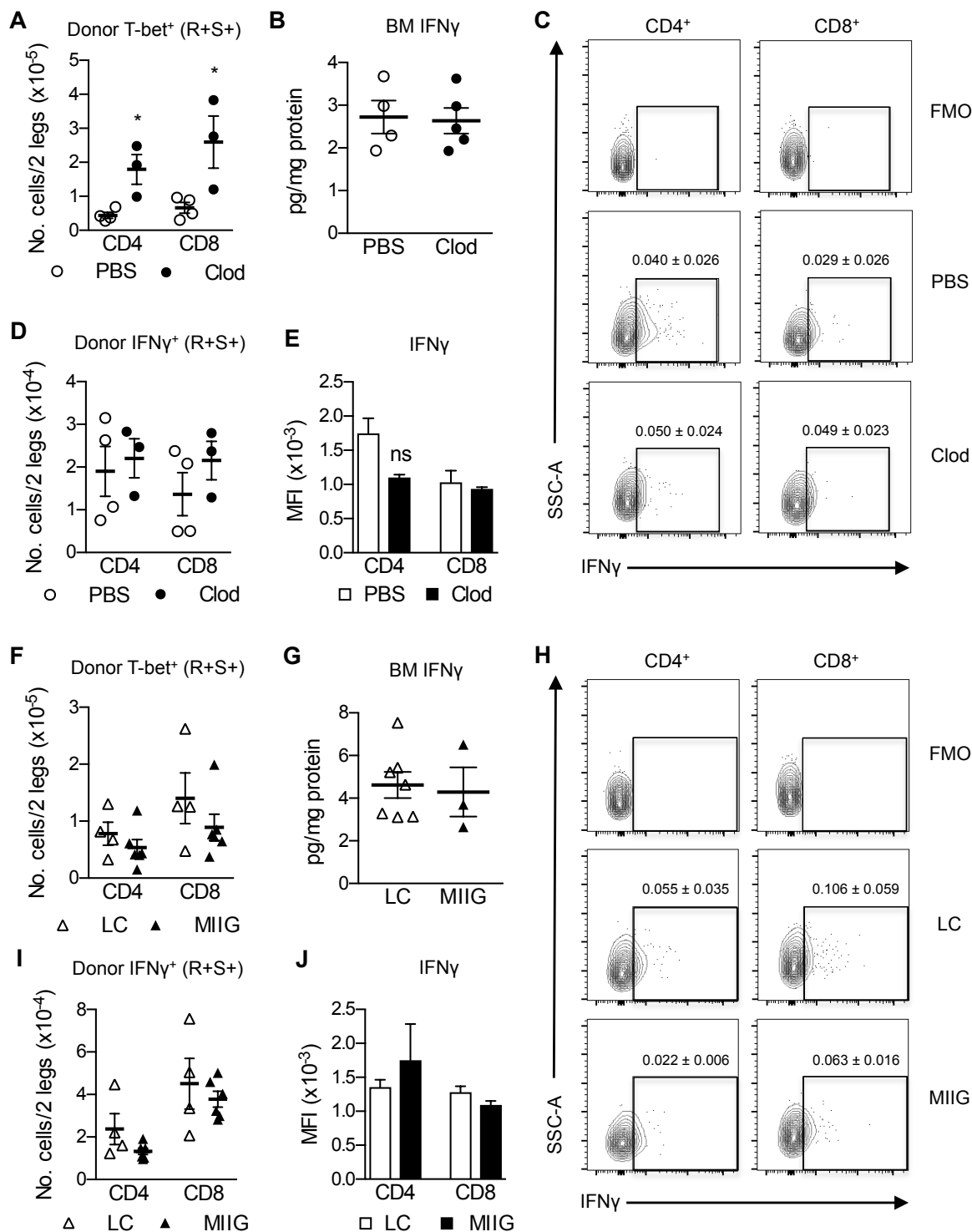
Supplemental Figure 2. Gating strategy for the analysis of BM resident macrophage populations. (A) Plots represent gating of BM myeloid cells from radiation control (top) and SAA (+Rad +Splenocytes; bottom) mice as follows: CD11b^{lo/-} MΦs (F4/80⁺ CD11b^{lo/-} SSC^{lo}; green gate), CD11b⁺ MΦs (F4/80⁺ CD11b⁺ Ly6C^{int} SSC^{lo}; blue gate), monocytes (CD11b⁺ Ly6C^{hi}; black gate), and neutrophils (CD11b⁺ F4/80⁻ Ly6G⁺; black gate). (B) Histograms represent surface protein expression of CD169 (top panel), Ly6G (middle panel), and VCAM1 (bottom panel) on CD11b^{lo/-} MΦs (green line), CD11b⁺ MΦs (blue line), or monocytes (black line). (C) The frequency of CD169⁺ MΦs (F4/80⁺ CD169⁺ SSC^{lo}) on days 8 and 14 post-radiation alone (□) or post-radiation and splenocyte transfer (■) is shown.



Supplemental Figure 3. HSC frequency and number are protected after M Φ targeting with clodronate liposomes or with M-CSFR antagonism during SAA. (A) SAA was induced and PBS- (○) or clod-lip (Clod; ●) was administered 1 day post-splenocyte transfer (p.s.t.). HSC frequency and number were enumerated on day 8 p.s.t. **(B)** M-CSFR antagonist (GW2580) or 10% DMSO vehicle was administered on days 4, 5, 6, and 7 (1 mg/mouse i.p. 2x/day) p.s.t. HSC frequency and number were enumerated in the BM on day 8 p.s.t. The mean \pm SEM is shown. Data represent one experiment repeated at least twice with 3-8 mice per group. Two-tailed student's t-test was used to compare between groups * $p < 0.05$, ** $p < 0.01$, *** $p < 0.005$.

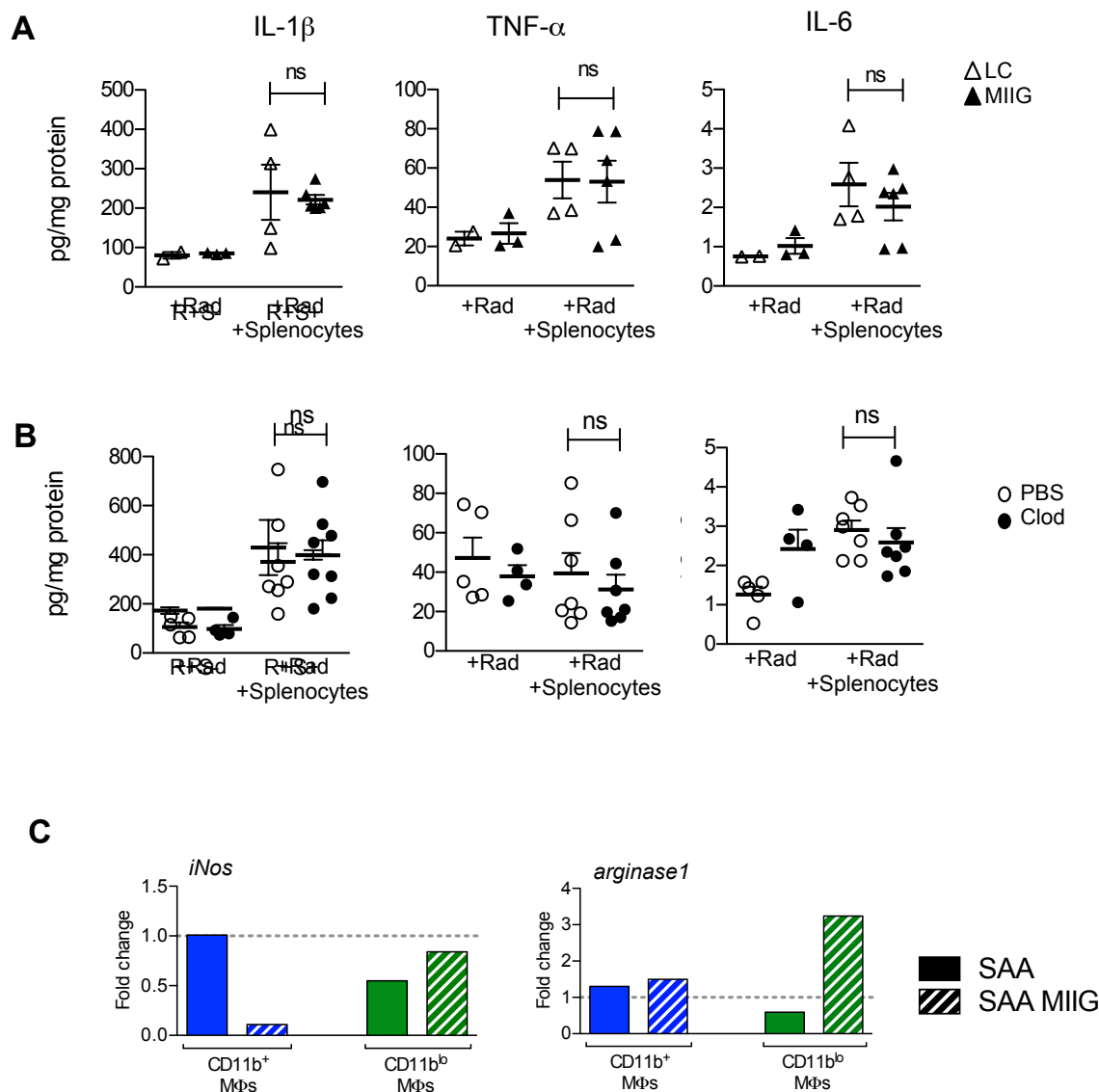


Supplemental Figure 4. Hematopoietic stem and progenitor cell numbers during SAA in MIIG mice and Clod-lip treated mice . (A) SAA was induced LC and MIIG F1 mice (top panels). SAA was induced in F1 mice and PBS- (○) or clod-lip (Clod; ●) was administered 1 day post-splenocyte transfer (p.s.t.; bottom panels). Bone marrow was harvested and analysed on day 8 p.s.t. **(A)** Numbers of phenotypic ST-HSCs (Lin- cKit+, CD135- CD150- CD48-), MPP2s (Lin- cKit+, CD135- CD150+ CD48+), and MPP3s (Lin- cKit+, CD135- CD150- CD48+) were assessed on day 8 p.s.t. **(B)** Numbers of phenotypic GMPs (Lin- cKit+ Sca1- FcγR+), phenotypic pre-CFU-E (Lin- cKit+ Sca1- CD105+ CD150+), phenotypic CFU-E (Lin- cKit+ Sca1- CD105+ CD150-) and MkPs (Lin- cKit+ Sca1- CD150+ CD41+) were evaluated on day 8 p.s.t.. Data represent one experiment with 3-4 mice per group. Two-tailed student's t-test was used to compare between groups * $p < 0.05$, ** $p < 0.01$



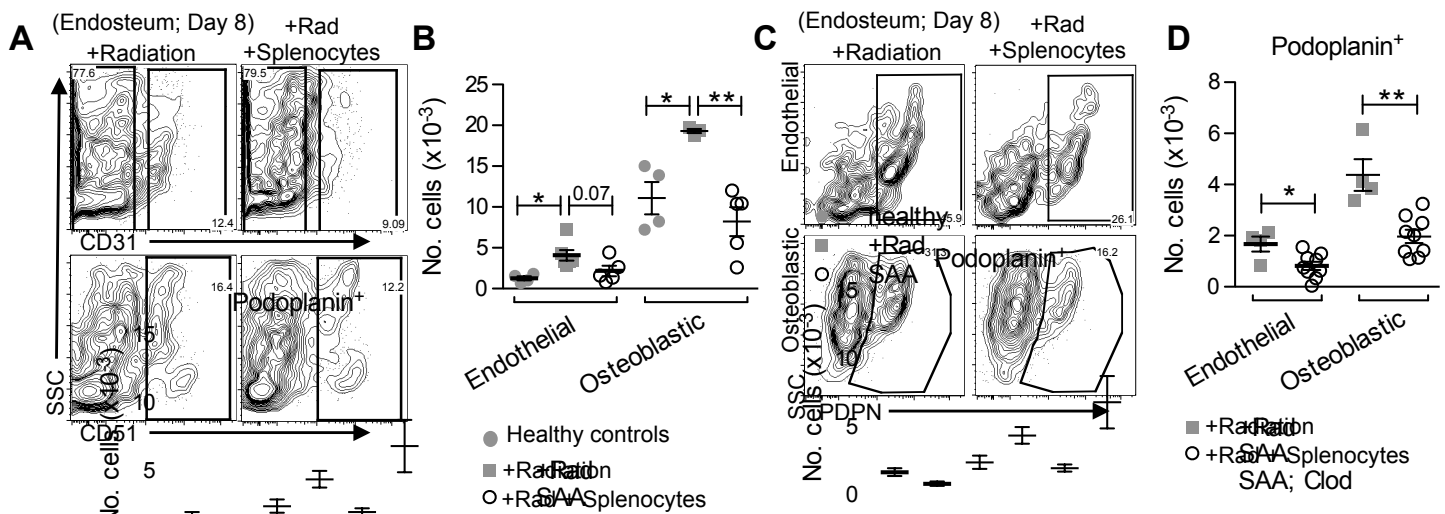
Supplemental Figure 5. Donor T cells and IFN- γ production are unaffected in clod-lip-treated and MIIG mice in SAA.

(A-E) SAA was induced, PBS- (○) or clod-lip (Clod; ●) was administered on day 1 post-splenocyte transfer (p.s.t.), and BM was analyzed on day 8 p.s.t. (A) Donor T-bet⁺ CD4⁺ and CD8⁺ lymphocytes were enumerated in the BM. (B) IFN γ protein was measured in the BM and normalized to total BM protein concentrations using a BCA protein assay kit. (C) Donor lymphocytes (GFP⁺ CD90⁺ CD4⁺/CD8⁺) were gated and plots represent IFN γ staining in CD4⁺ (left) and CD8⁺ (right) donor lymphocytes derived from PBS-lip (middle) and clod-lip (bottom) SAA mice, relative to fluorescence minus one (FMO) controls (top). (D-E) Graphs represent donor IFN γ ⁺ CD4⁺ and CD8⁺ lymphocyte numbers (D) and IFN γ MFI (E). (F-J) SAA was induced in LC and MIIG mice and BM was analyzed on day 8 p.s.t. (F) Donor T-bet⁺ CD4⁺ and CD8⁺ lymphocytes were enumerated in the BM. (G) IFN γ protein was measured, as described in (B). (H) Donor lymphocytes were gated and plots represent IFN γ staining in CD4⁺ (left) and CD8⁺ (right) donor lymphocytes derived from LC (middle) and MIIG (bottom) SAA mice. (I-J) Graphs represent donor IFN γ ⁺ CD4⁺ and CD8⁺ lymphocyte numbers (I) and IFN γ MFI (J). The mean \pm SEM is shown. Two-tailed student's t-test was used to compare between groups. * $p < 0.05$.



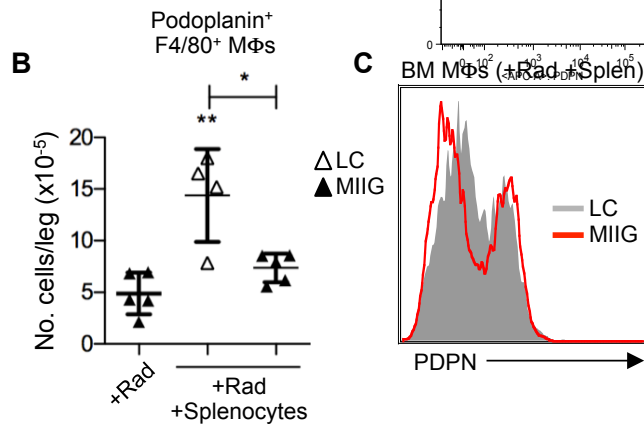
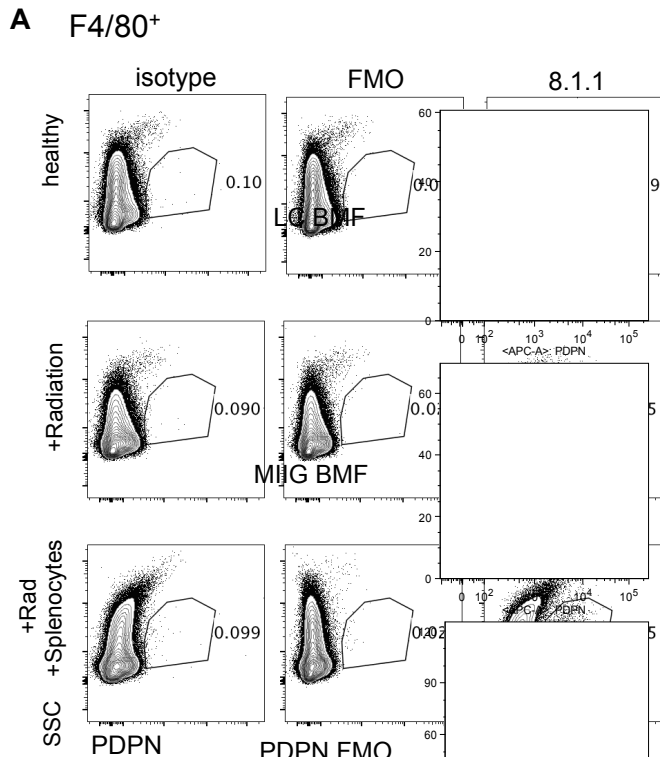
Supplemental Figure 6. Inflammatory cytokine profile in the bone marrow during SAA.

Bone marrow homogenates were collected from radiation control (+Rad) and SAA (+Rad +Splenocytes) mice on day 8 post-induction. Protein analysis was performed using an inflammatory cytokine luminex panel. **(A)** Graphs represent MIIG (\blacktriangle) and LC (Δ) levels of the indicated cytokines. **(B)** Graphs represent levels of the indicated cytokines in the BM of radiation control (+Rad) and SAA (+Rad +Splenocytes) mice that received PBS- (\circ) or clod-lip (Clod; \bullet) 1 day post-induction. Values were normalized to total protein in the BM for each sample using a BCA protein assay kit. Data represent one experiment with 3-5 mice/group. The mean \pm SEM is shown. Two-tailed student's t-test was used to compare between groups ** $p < 0.01$, *** $p < 0.001$. **(C)** Sort purified M ϕ s were obtained on day 8 post SAA induction from LC and SAA MIIG mice and evaluated for expression of *iNos* and *arginase1*. Data is normalized to CD11b⁺ M ϕ s from LC SAA mice. Data come from two independent experiments and two independent sorts, reflecting at least 3 individual mice.

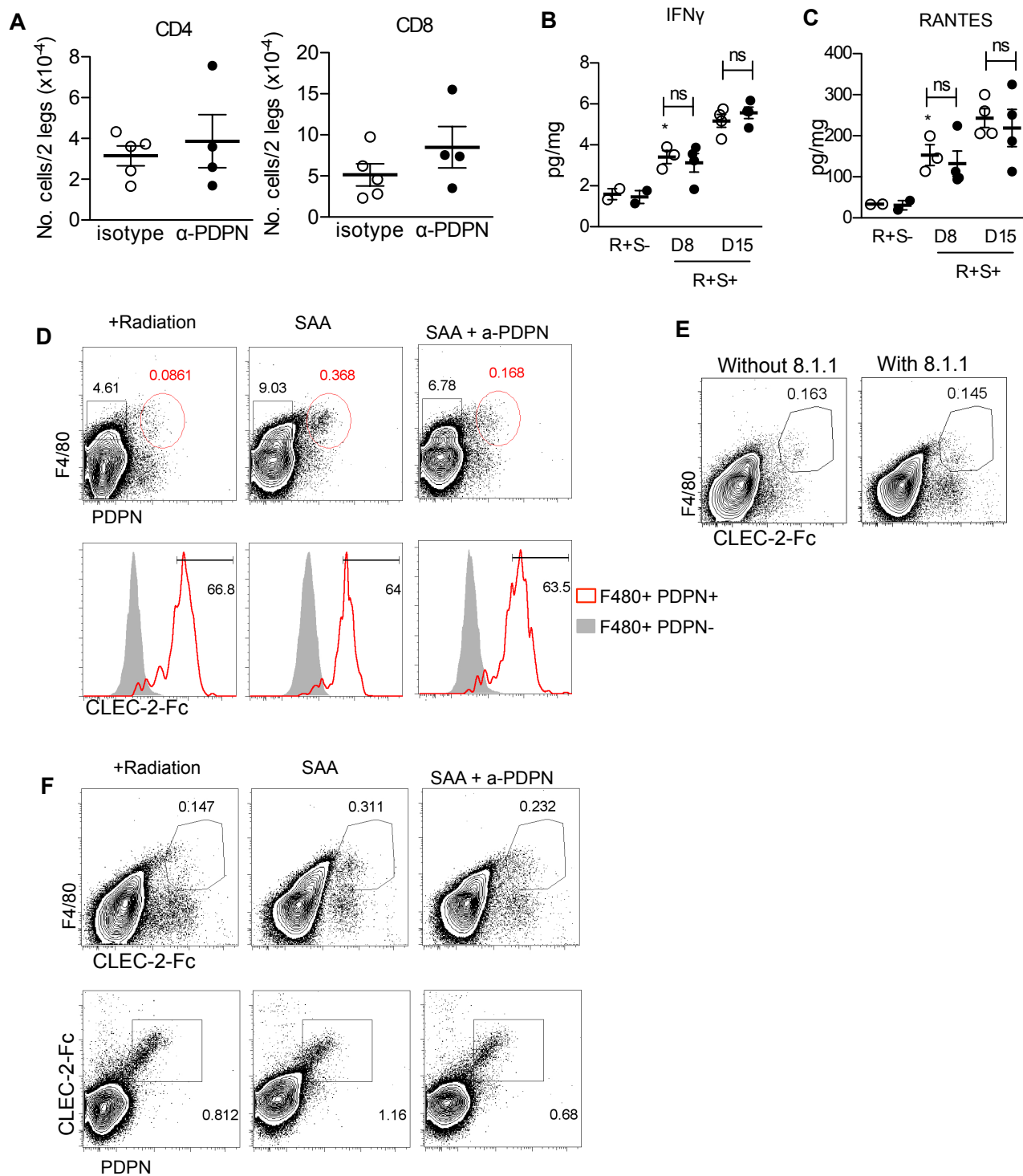


Supplemental Figure 7. Non-hematopoietic bone-associated cells are reduced during SAA

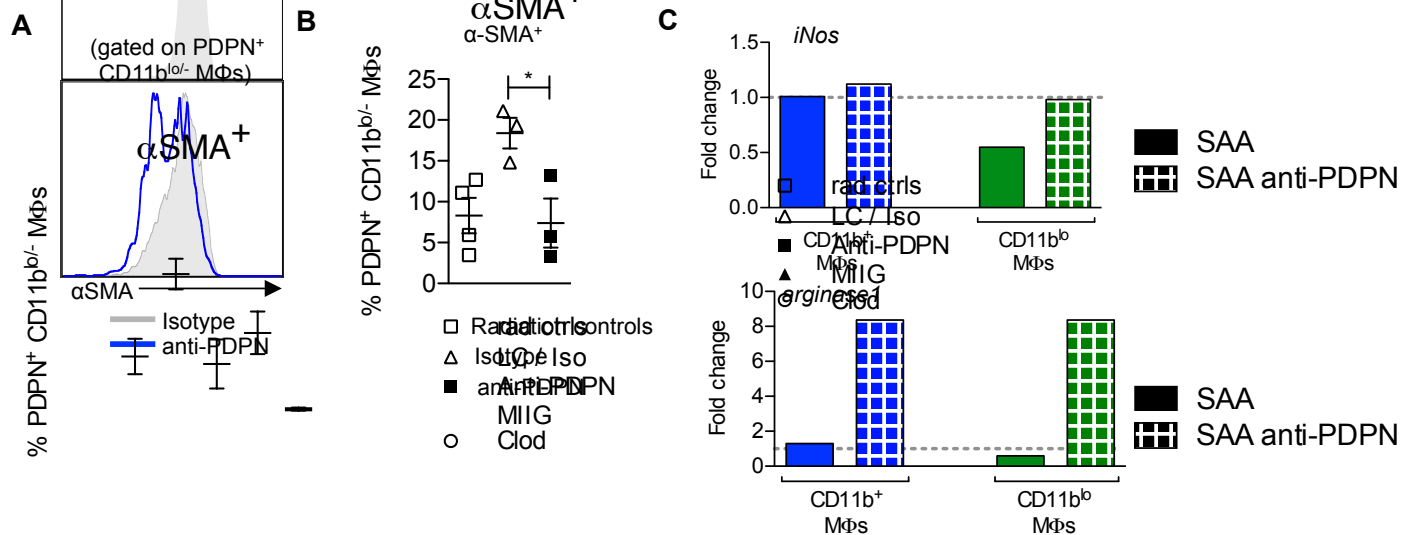
Bone associated cells were collected from radiation control (+Rad) and SAA (+Rad +Splenocytes) mice on day 8 post-induction by enzymatic digestion. **(A)** Flow cytometric plots represent the identification of endothelial cells (CD31⁺; top) gated on non-hematopoietic (CD45⁻ Ter119⁻) endosteal-associated cells, and osteoblastic cells (CD51⁺; bottom) gated on non-hematopoietic, non-endothelial (CD45⁻ Ter119⁻ CD31⁻) endosteal cells. Numbers indicate frequency of parent populations. **(B)** Graph represents endothelial and osteoblastic cell numbers per pair of hindlimbs or coxal bones in healthy, non-irradiated mice (gray circles), radiation control (gray squares), and SAA mice (open circles). **(C)** Flow cytometric plots represent the expression of Podoplanin (PDPN) among total endothelial and osteoblastic endosteal-associated cells in radiation control (gray squares) and SAA mice (open circles). **(D)** Graph represents the number of PDPN-expressing endothelial and osteoblastic endosteal-associated cells in radiation control and SAA mice. Data represent 2-3 experiments with 3-9 mice/group. The mean \pm SEM is shown. Two-tailed student's t-test was used to compare between groups **p<0.01, ***p<0.001.



Supplemental Figure 8. Expression of podoplanin on macrophages. (A) Flow cytometric analysis of podoplanin expression. BM was analyzed for F4/80⁺ cells and podoplanin (PDPN) staining with the 8.1.1 clone (right column) was compared to the isotype control (left column) and fluorescence minus one (FMO) control (middle column), under healthy and radiation control conditions, and SAA (+Rad +Splenocytes) conditions. Graphs represent (B) PDPN⁺ MΦ numbers and (C) MΦ PDPN expression at day 8 post-splenocyte transfer (p.s.t.) in SAA MIIG (▲) and LC (Δ) mice



Supplemental Figure 9. Impact of anti-podoplanin (8.1.1) administration during SAA. (A) Tbet⁺ CD4 and CD8 T cells were enumerated in the BM of SAA-induced mice treated with isotype (○) or anti-PDPN antibody (α-PDPN; ●) on day 8 p.s.t. (B) IFN γ protein levels were measured at days 8 and 15 p.s.t. in the BM of radiation control and SAA mice treated with anti-PDPN (α-PDPN; ●) or isotype control (○) antibodies. (C) RANTES protein levels were measured at days 8 and 15 p.s.t. in the BM of radiation control and SAA mice treated with anti-PDPN (α-PDPN; ●) or isotype control (○) antibodies. Protein levels were normalized to total BM protein concentrations using a BCA protein assay kit. (D) Binding of CLEC-2-Fc fusion to BM cells from radiation control, SAA, and SAA mice treated with anti-PDPN. Top row shows PDPN and F4/80 expression, second row shows CLEC-2 binding on F4/80+ PDPN- (gray, filled histograms) and F4/80+PDPN+ populations (red, open histograms). (E) Clec-2 binding is shown in samples treated with and without addition of 8.1.1. (F) The percentage of F4/80+ CLEC-2 bound cells in the respective groups (top row) and cells analyzed for both CLEC-2 and PDPN (bottom row).



Supplemental Figure 10. Anti-podoplanin antibody (8.1.1) modulates MΦ phenotype and function during SAA. (A) Histogram of αSMA expression in PDPN⁺ CD11b^{lo/-} MΦs 8 d.p.s.t.. (B) Frequencies of αSMA positive cells among CD11b^{lo/-} MΦs in radiation controls, SAA, and SAA + α-PDPN-treated mice. Data represent one experiment with 3-5 mice/group. The mean ± SEM is shown. Two-tailed student's t-test was used to compare between groups *p<0.05. (C) Sort purified MΦs were obtained on day 8 post SAA induction from control and anti-PDPN treated mice and evaluated for expression of *iNos* and *arginase1*. Data is normalized to CD11b⁺ MΦs from wildtype, isotype-treated SAA mice. Data are from two independent experiments, two independent sorts, and reflect at least 3 individual mice.